SNOW PROBE FOR *IN SITU* DETERMINATION OF WETNESS AND DENSITY

Technical Report
U.S. Army Research Office
DAAL 03-92-G-0269

John R. Kendra
Fawwaz T. Ulaby
Kamal Sarabandi

Radiation Laboratory
Department of Electrical Engineering and Computer Science
The University of Michigan

June 1993

Abstract

The amount of water present in liquid form in a snowpack exercises a strong influence on the radar and radiometric responses of snow. Conventional techniques for measuring the liquid water content m_v suffer from various shortcomings, which include poor accuracy, long analysis time, poor spatial resolution, and/or cumbersome and inconvenient procedures. This report describes the development of an improved design of the "Snow Fork", a hand-held electromagnetic sensor that was introduced by Sihvola and Tiuri [1], for quick and easy determination of snow liquid water content and density. The novel design of this sensor affords several important advantages over existing similar sensors. Among these are improved spatial resolution and accuracy, and reduced sensitivity to interference by objects or media outside the sample volume of the sensor. The sensor actually measures the complex dielectric constant of the snow medium, from which the water content and density are obtained through the use of semi-empirical relations. To confirm the validity of these relations, it was necessary to conduct comparisons against reliable and accurate *direct* techniques. For liquid water determination, two direct procedures were investigated: freezing calorimetry and dilatometry. Of these only the freezing calorimeter was judged suitable. An extensive comparison study was then carried out between it and the snow probe. Through this comparison, the following specifications were established for the snow probe: (1) liquid water content measurement accuracy = ± 0.66 % in the wetness range from 0 to 10% by volume and (2) wet snow density measurement accuracy = ± 0.03 g/cm^3 in the density range from 0.1 to 0.6 g/cm^3. In addition, it was found that the existing semi-empirical expressions relating dielectric constant to the snow physical parameters fail to agree with experimental observations when the snow liquid water content exceeds $\approx$ 3%. Accordingly, the expression was modified to correctly model the observed behavior.

Contents

List of Figures

List of Tables

1 Introduction

In the study of microwave remote sensing of snow, it is necessary to consider the presence of liquid water in the snowpack. The dielectric constant of water is large (e.g., $\epsilon_w = 88 - j9.8$ at 1 GHz [1]) relative to that of ice ($\epsilon_i \approx 3.15 - j0.001$ [2]), and therefore even a very small amount of water will cause a substantial change in the overall dielectric properties of the snow medium, particularly with respect to the imaginary part. These changes will, in turn, influence the radar backscatter and microwave emission responses of the snowpack.

Among instruments available for measuring the volumetric liquid-water content of snow, m_v, under field conditions, the freezing calorimeter [3, 5, 6] offers the best accuracy ($\approx 1\%$) and is one of the more widely used in support of quantitative snow-research investigations. In practice, however, the freezing calorimeter technique suffers from a number of drawbacks. First, the time required to perform an individual measurement of m_v is on the order of thirty minutes. Improving the temporal resolution to a shorter interval would require the use of multiple instruments, thereby increasing the cost and necessary manpower. Second, the technique is rather involved, requiring the use of a freezing agent and the careful execution of several steps. Third, the freezing calorimeter actually measures the mass fraction of liquid water in the snow sample, W, not the volumetric water content m_v. To convert W to m_v, a separate measurement of snow density is required. Fourth, because a relatively large snow sample (on the order of 250 cm^3) is needed in order to achieve acceptable measurement accuracy, it is difficult to obtain the sample from a thin horizontal layer, thereby rendering the technique impractical for profiling the variation of m_v with depth. Yet, the depth profile of m_v, which can exhibit rapid spatial and temporal variations [7, 8], is one of the most important parameters of a snowpack, both in terms of the snowpack hydrology and in terms of the effect that m_v has on the microwave emission and scattering behavior of the snow layer.

In experimental investigations of the radar response of snow-covered ground, it is essential to measure the depth profile of m_v with good spatial resolution (on the order of 2-3 cm) and adequate temporal resolution (on the order of a few minutes), particularly during the rapid melt and freeze intervals of the diurnal cycle. Examination of available techniques narrowed the list to two potential instruments: (a) the dilatometer, which measures the change in

volume that occurs as a sample melts completely, and (b) the "Snow Fork", which is a microwave instrument that was developed in Finland [1]. As discussed in Appendix A of the report, the dilatometer approach was rejected because of poor measurement accuracy and long measurement time (about one hour). In the process of examining the Snow Fork approach, we decided to modify the basic design in order to improve the sensitivity of the instrument to m_v and reduce the effective sampled volume of the snow medium, thereby improving the spatial resolution of the sensor. Our modified design, which we shall refer to as the "snow probe" is described in Section 2. The snow probe measures the real and imaginary parts of the relative dielectric constant of the snow medium, from which the liquid water content m_v and the snow density ρ_s are calculated through the use of semi-empirical relations that had been established by Hallikainen *et al.* [2] and by Sihvola and Tiuri [1]. To evaluate the performance of the snow probe, independent measurements of density were performed using a standard tube of known volume, whose weight is measured both empty and when full of snow, and of m_v using a freezing calorimeter. One of the unexpected by-products of this study was the discovery that the semi-empirical relations developed by Hallikainen *et al.* [2] are not valid over the full ranges of snow wetness and density. Consequently, a modified set of expressions is proposed instead, as discussed in Section 3.

2 Snow Dielectric Probe

2.1 Snow Probe Measurement System

Figures 1 and 2 show a photograph of the snow probe measurement system, and a schematic of the same, respectively. The sweep oscillator, under computer control, sweeps (in discrete 10 MHz steps) over a relatively large frequency range. This serves to determine, within ± 5 MHz, the frequency at which the detected voltage is a maximum, corresponding to the resonance frequency of the probe. The RF power transmitted thru the snow probe is converted to video by the crystal detector, measured by the voltmeter, which in turn sends the voltage values to the computer. The frequency spectrum is generated in real-time on the monitor of the computer. In the second pass, a much narrower frequency range is centered around the peak location and

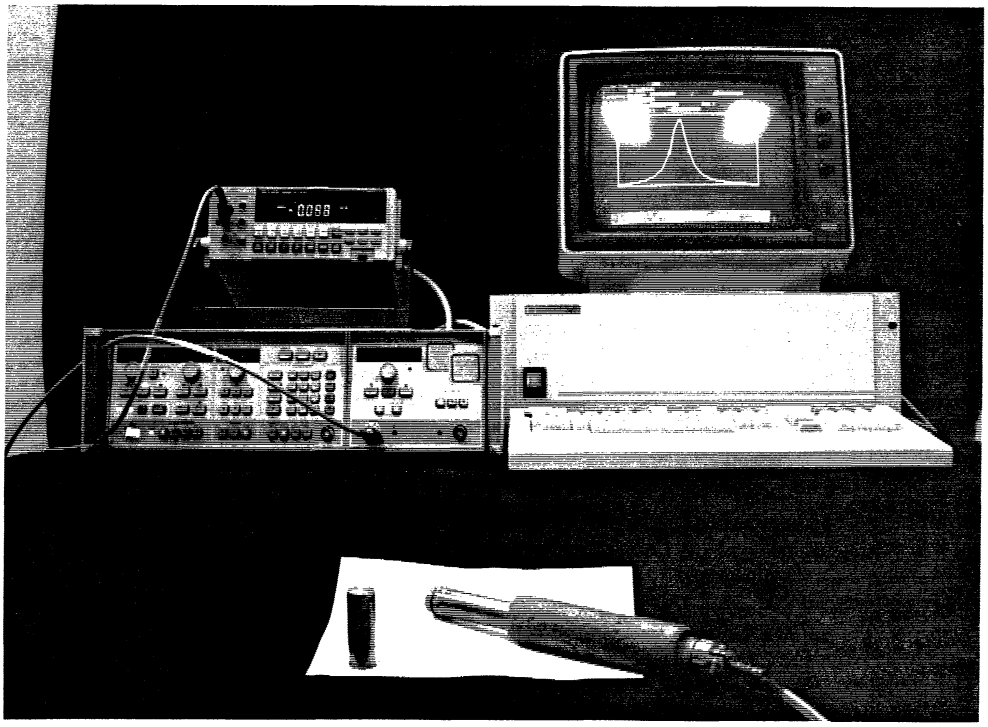

Figure 1: Photograph of snow probe system.

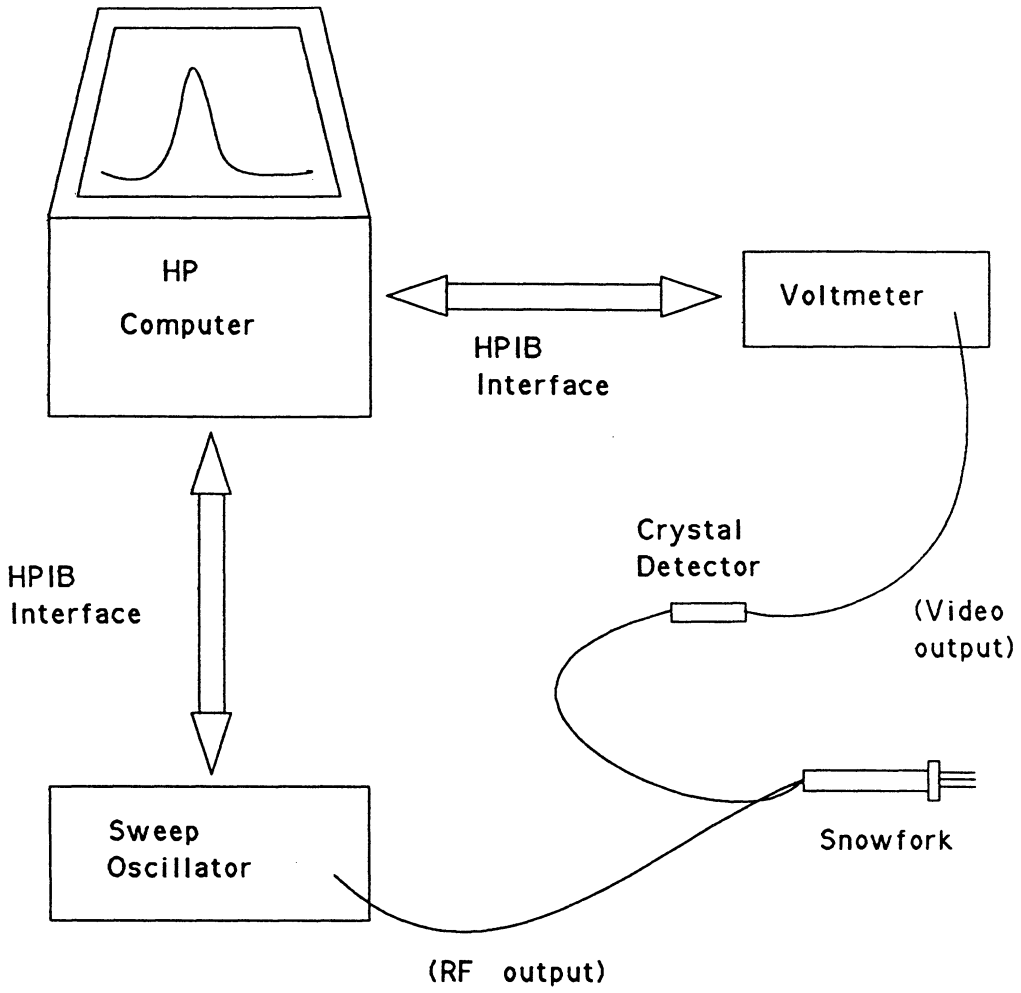

Figure 2: Schematic of snow probe system.

swept over with a finer step size ($\approx$ 1 MHz). The center frequency and the 3-dB bandwidth around it are found, and from these, first the dielectric constant and then the snow parameters m_v and ρ_s are determined according to procedures described in detail in Section 3 of this report.

2.2 Sensor Design

The snow probe is essentially a transmission-type electromagnetic resonator. The resonant structure used in the original design [1] was a twin-pronged fork. This structure behaves as a two wire transmission line shorted on one end and open on the other. It is resonant at the frequency for which the length of the resonant structure is $\lambda/4$ in the surrounding medium. The RF power is fed in and out of the structure using coupling loops.

For our design, we used a coaxial type resonator, as illustrated in Figure 3. The skeleton of the outer conductor is achieved using four prongs. The principle is basically the same: a quarter wavelength cavity, open on one end, shorted on the other, with power delivered in and out through coupling loops. The coaxial design was chosen for purposes of spatial resolution. Being a shielded design, the electric field is confined to the volume contained within the resonant cavity, as opposed to the original design, which used only two prongs. The coaxial design also had a much higher quality factor, ($\approx$ 120 *vs.* 40 – 70 for the original design) which, as discussed below, allows for more accurate determination of the complex dielectric constant. A photograph of the snow probe is shown in Figure 4.

The real part of the dielectric constant is determined by the resonant frequency of the transmission spectrum, or equivalently, the frequency at which maximum transmission occurs. As mentioned above, this corresponds to the frequency for which the wavelength *in the medium* is equal to four times the length of the resonator. If the measured resonant frequency is f_a in air and f_s in snow, then the real part of the dielectric constant is given by

$$\epsilon_s' = \left(\frac{f_a}{f_s}\right)^2. \tag{1}$$

The imaginary part of ϵ_s is determined from the change in Q, the quality factor of the resonator. The quality factor is defined as follows [9]:

$$Q = \frac{\omega(\text{time-average energy stored in system})}{\text{energy loss per second in system}}, \tag{2}$$

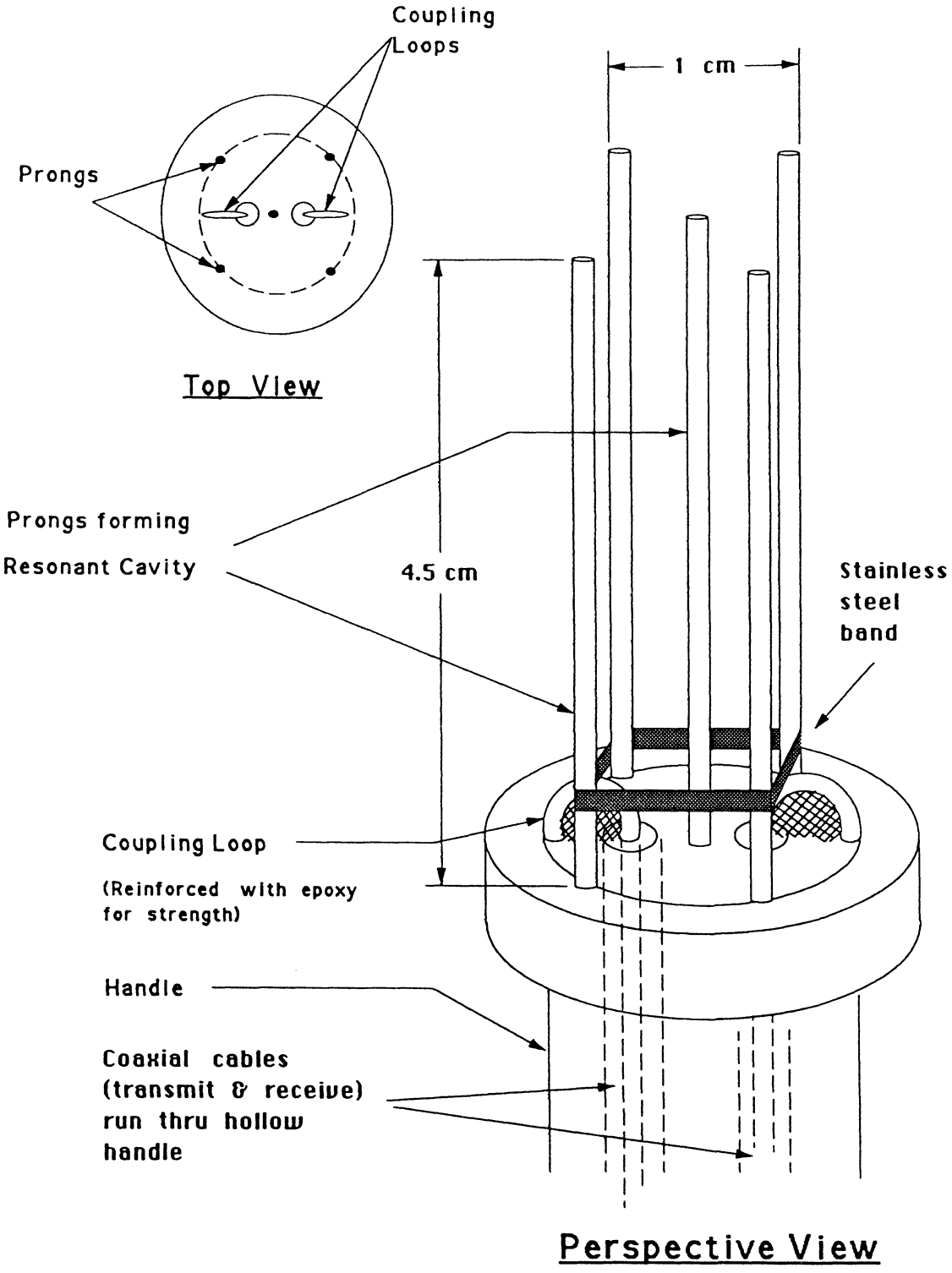

Figure 3: Illustration of Snow Probe. Coaxial transmission lines extend through handle. At the face of the snow probe, the center conductors of the coaxial lines extend beyond and curl over to form coupling loops.

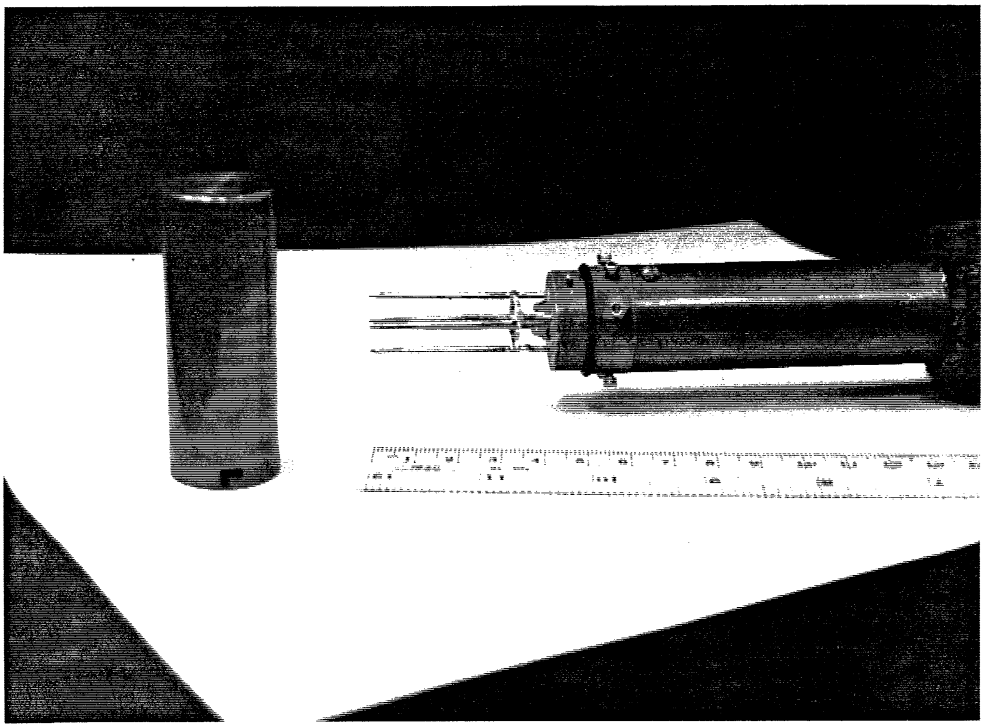

Figure 4: Photograph of snow probe with cap.

and it may be determined by measuring Δf, the half-power bandwidth [9]:

$$Q = \frac{\Delta f}{f_o} , \tag{3}$$

where f_o is the resonant frequency (f_a or f_s, depending on whether the medium is air or snow). In the case of the snow probe, power losses exist due to radiation, coupling mechanisms (ie. coupling loops), and to dissipation in a lossy dielectric. Thus the measured Q is given by:

$$\frac{1}{Q_m} = \frac{1}{Q_{R_\epsilon}} + \frac{1}{Q_d} , \tag{4}$$

where Q_m is the measured Q when the probe is inserted in the snow medium, Q_{R_ϵ} is the quality factor describing both the radiation losses and the power losses due to the external coupling mechanisms for the dielectric-filled snow probe, and Q_d pertains to the dielectic losses. It has been shown [9] that

$$\frac{1}{Q_d} = \tan\delta = \frac{\epsilon''}{\epsilon'} . \tag{5}$$

As can be seen from (4) and (5), in order to calculate ϵ'' one must not only measure Q_m and know ϵ', but the value of Q_{R_ϵ} should be available also. As long as $\tan\delta$ is very small, we may assume that Q_{R_ϵ}, which is related to the power radiated by the snow probe, is a function of the real part of ϵ only. We can therefore define experimentally the functional dependence of Q_{R_ϵ} on ϵ', and then, for the actual test materials, having found ϵ' from the *shift* alone in the resonance curve, specify Q_{R_ϵ} and hence compute ϵ''. The details of how the snow probe was characterized are given in the next sub-section.

We noted at the beginning of this section that our coaxial design for the snow probe had a considerably higher Q than the original twin-prong design. Why this increases the precision of the dielectric measurements may be understood from an examination of the relations already cited in this section. A high Q means a sharper resonance, and thus greater precision in determining the center frequency f_s, and from (1), ϵ'. From equations (4) and (5) it is seen that ϵ'' is determined from the contribution of the dielectric power loss to the total power loss. As the radiated power increases (Q_{R_ϵ} decreases), the contribution of the dielectric loss becomes an increasingly smaller fraction of the total power loss. Thus a small change in dielectric loss, or equivalently, a small change in $\frac{1}{Q_d} = \tan\delta = \epsilon''/\epsilon'$, becomes more difficult to detect from the measured Q.

2.3 Characterization of Snow Probe

In order to compute the functional dependence of Q_{R_ϵ} on ϵ', it was necessary to determine very precisely the complex dielectric constants of a variety of materials. This was achieved using an L-band cavity resonator. The materials used were sand, sugar, coffee, wax, and of course, air. The cavity used was cylindrical in shape with a diameter of 13.9 cm and a height of 6.35 cm. Details of how the dielectric constant of a material is determined using such a cavity are given in Appendix B.

We now recall equation (4) which pertains to Q of the snow probe:

$$\frac{1}{Q_m} = \frac{1}{Q_{R_\epsilon}} + \frac{\epsilon''}{\epsilon'} .$$

Once Q_m is measured for our calibration materials, exact knowledge of the loss tangent for a given material allows isolation of the quantity Q_{R_ϵ}. The quantity Q_{R_ϵ} is equivalent to Q_m for a *lossless* material having dielectric constant ϵ'. That is, for such a lossless material,

$$\frac{1}{Q_m} = \frac{1}{Q_{R_\epsilon}} = \frac{\Delta f_{\delta=0}}{f_r}. \tag{6}$$

The quantity $\Delta f_{\delta=0}$ is thus the 3-dB bandwidth of the resonance spectrum of the snow probe when immersed in a lossless material having dielectric constant ϵ'. From our measurements of the five calibration materials, the quantity $\Delta f_{\delta=0}$ was found to be a linear function of the resonant frequency. Information pertaining to the analysis of the calibration materials is given in Table 1, and a plot of $\Delta f_{\delta=0}$ *versus* f_r is given in Figure 5. Figure 5 also shows (triangles) the 3-dB bandwidths of each of the calibration materials before the effect of the dielectric losses was removed. We rewrite (4) to reflect the linear dependence of $\Delta f_{\delta=0}$ on f_r:

$$\frac{1}{Q_m} = \frac{\Delta f}{f_r} = \frac{m f_r + b}{f_r} + \frac{\epsilon''}{\epsilon'}, \tag{7}$$

where m and b are the slope and intercept respectively of the line in Figure 5 relating $\Delta f_{\delta=0}$ to f_r. Invoking (1) allows us to write,

$$\Delta f = m f_r + b + \frac{f_r^3 \epsilon''}{f_a^2} \tag{8}$$

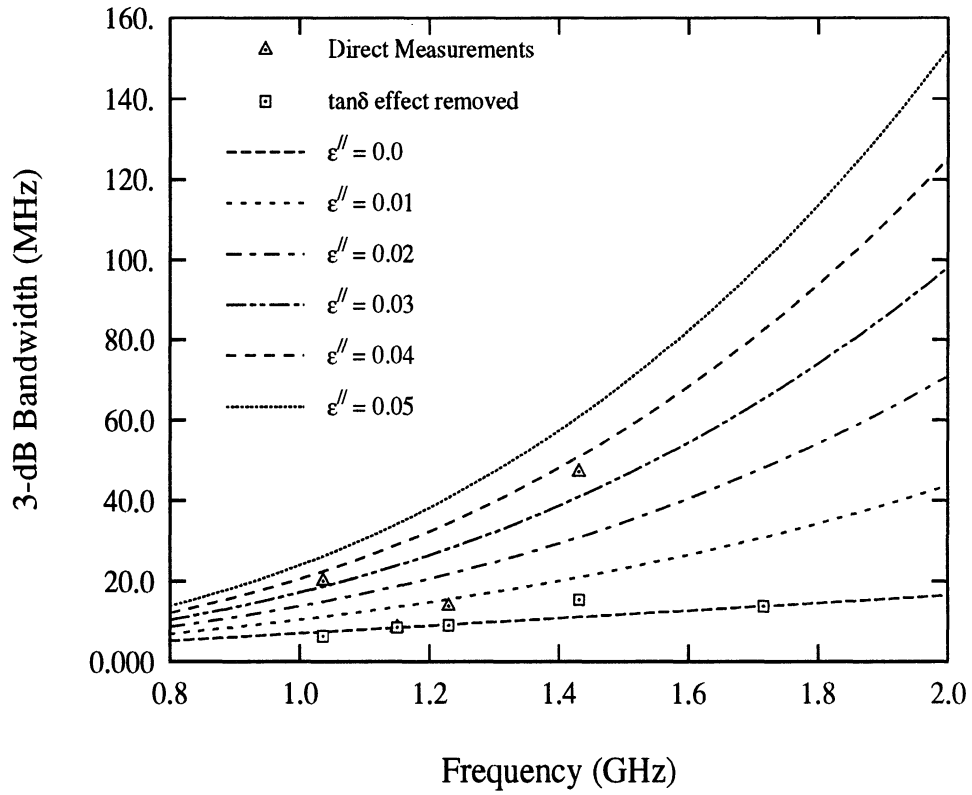

Figure 5: Snow probe resonance bandwidth as a function of permittivity. Marks ($\triangle$) represent 3-dB bandwidth of materials (lowest freq. to highest) sand, wax, sugar, and coffee. Squares represent bandwidth of resonances if materials are lossless ($\epsilon'' = 0$).

Material	$\bar{\epsilon}$	(GHz) f_R	Q_m	(MHz) $\Delta f_{\delta=0}$
Air	$1.0 - j0.0$	1.715776	125.2	13.700
Sand	$2.779 - j3.7e^{-2}$	1.036	51.7	6.245
Sugar	$1.984 - j7.778e^{-3}$	1.22947	89.3	8.947
Coffee	$1.497 - j3.32e^{-2}$	1.43125	30.4	15.339
Wax	$2.26 - j2.9e^{-4}$	1.150308	137.0	7.853

Table 1: 3-dB bandwidth of Snow Probe as a function of ϵ_r (real part of permittivity).

where f_a is the resonant frequency of the device in air. We have made use of (8) in Figure 5 to generate curves of Δf for particular values of ϵ''.

It is clear from (7) that, given a measured Q_m and resonant frequency f_r and given knowledge of the constants m and b, ϵ'' may be directly calculated as follows:

$$\epsilon'' = \left(\frac{f_a}{f_r}\right)^2 \left[\frac{1}{Q_m} - (m + \frac{b}{f_r})\right]. \tag{9}$$

The determination of the function parameters m and b therefore constitutes the "calibration" of the probe. In general, we expect this calibration to be valid as long as nothing occurs which might affect the radiating or power input/output characteristics of the device. However, if we assume that the function of $\Delta f_{\delta=0}$ *versus* f_r is always a linear one, re-calibration may be performed at any time by measuring just two materials for which the dielectric constant is known exactly. In practice, we calibrate the device daily when used, by measuring air and heptane ($\tilde{\epsilon} = 1.925 - j0.8 \times 10^{-4}$). Generally the calibration coefficients are reproduced quite closely, and the daily calibration is done mainly as a precaution. A typical calibration curve is,

$$\Delta f(\text{MHz}) = 8.381 \times f(\text{GHz}) + 0.7426 \tag{10}$$

The determination of dielectric constant with the snow probe is summarized as follows: parameters m and b are obtained by measuring the Q of two materials of known dielectric constant (air and heptane) and then applying (8); ϵ' is obtained from the shift in resonance relative to air (equation (1)); and finally, ϵ'' is computed from (9).

2.4 Spatial Resolution / Outside Interference

As mentioned earlier, the partially shielded design of this sensor reduces its sensitivity to permittivity variations outside the sample volume. By sample volume, we refer to the volume inside the cylinder described by the four outside prongs (Figure 3). The coaxial design will tend to produce greater field confinement relative to a twin-prong structure.

The effective sample volume was tested in the following way: a cardboard box (30cm $\times$ 30cm) was filled with sugar to a depth of $\approx$ 16 cm. The snow probe was inserted into the sugar at a position in the center of the top surface, and then the dielectric constant was measured. Next, a thin metal plate ($\approx$ 25 cm square) was inserted into the sugar, parallel to and resting against one side of the box. The dielectric constant was re-measured. The metal plate was incrementally moved closer to the sensor position, with dielectric measurements recorded at each sensor-to-plate distance. The results of the experiment are shown in Figure 6, in which ϵ'' is plotted as a function of the sensor-to-plate separation. The plate appears to have a weak influence on the measurement, even at a distance of only 0.6 centimeters. To put this variation into perspective, had the material been snow, and using the relations given in section 3.1, the fluctuation in the estimate of liquid water would have ranged from $m_v = 0.6\%$ to $m_v = 0.8\%$. The real part of the dielectric constant (not shown in Figure 6) stayed within the range 2.00 - 2.01 during the experiment. The results of this experiment, which essentially confirm the expectation that the electric field is confined to the volume enclosed by the four prongs, translate into a vertical resolution on the order of 2 cm when the snow probe is inserted into the snowpack horizontally (the snow probe cross section is 1cm $\times$ 1cm).

3 Liquid Water Content and Density Retrieval

3.1 Procedure

The volumetric liquid water content, m_v, and the snow density ρ_s can be calculated from the complex dielectric constant ϵ (and knowledge of the exact frequency at which it was measured) using a set of semi-empirical relation-

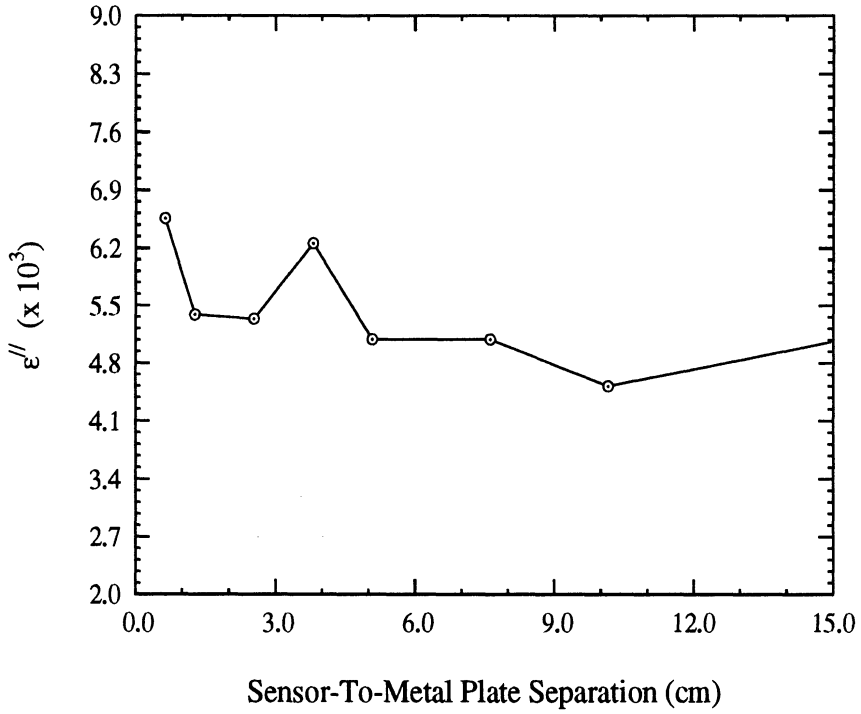

Figure 6: Variation in measurement of ϵ'' of sugar as a function of sensor proximity to metal plate. (Real part ϵ' stayed in the range 2.00 - 2.01.)

ships [1, 2]. These equations are:

$$\epsilon'_{ds} = 1 + 1.7\rho_{ds} + 0.7\rho_{ds}^2 \tag{11}$$

$$\Delta\epsilon'_{ws} = \epsilon'_{ws} - \epsilon'_{ds} = 0.02m_v^{1.015} + \frac{0.073m_v^{1.31}}{1 + (f/f_w)^2} \tag{12}$$

$$\epsilon''_{ws} = \frac{0.075(f/f_w)m_v^{1.31}}{1 + (f/f_w)^2} \tag{13}$$

where:

ϵ'_{ds} = the real part of the dielectric constant of dry snow,
ρ_d = the "dry density" of snow, which would result if all the volume occupied by water was replaced with air,
ϵ'_{ws} = the real part of wet-snow dielectric constant
ϵ'_{ds} = the real part of dry-snow dielectric constant,
m_v = the volumetric liquid water content (%),
f_w = 9.07 GHz (related to relaxation frequency of water at 0° C),
f = frequency (GHz) at which ϵ_{ws} is determined.

Equation (11), from [1], relates the real part of the dielectric constant of *dry snow* to its density. Equations (12) and (13), from [2], are semi-empirical Debye-like equations.

Upon measuring ϵ''_{ws} (by the snow probe), m_v can be calculated directly from (13):

$$m_v = \left\{ \frac{\epsilon''_{ws}\,[1 + (f/f_w)^2]}{0.075(f/f_w)} \right\}^{\frac{1}{1.31}}. \tag{14}$$

Note that (13) basically relates ϵ''_{ws} to the imaginary part of the dielectric constant of water, ϵ''_w, scaled by its volume fraction in the snow mixture, m_v. This follows from the fact that $\epsilon''_a = 0$ for the air constituent and ϵ''_i of the ice constituent is several orders of magnitude smaller than ϵ''_w of water.

From (11) and (12) we may compute ϵ'_{ds} as follows:

$$\epsilon'_{ds} = \epsilon'_{ws} - 0.02m_v^{1.015} - \frac{0.073m_v^{1.31}}{1 + (f/f_o)^2}. \tag{15}$$

Then from (11) and (15) we can compute ρ_{ds} from the quadratic equation:

$$\rho_{ds} = -1.214 + \sqrt{1.474 - 1.428(1 - \epsilon'_{ds})}, \tag{16}$$

in which only the positive root is considered.

The the dry snow density ρ_{ds}, and the volumetric liquid water content m_v (%) are related to the the wet snow density ρ_{ws} by [4]:

$$\rho_{ws} = \rho_{ds} + \frac{m_v}{100.}. \tag{17}$$

3.2 Results

Since the physical snow parameters yielded by the snow probe are the results of empirical and semi-empirical equations, it was necessary to see how closely the snow probe reproduced the results obtained from well-established direct techniques. The parameters tested were density and liquid water content. The direct techniques used were a simple gravimetric density measurement and freezing calorimetry for liquid water.

It should be noted that the relations used with the snow probe (given in (11),(12), and (13)) deal with liquid water *volume* fraction, m_v. The freezing calorimeter, however, produces liquid water *mass* fraction (W) as its output. In order to compare m_v as measured by the snow probe with W as measured by the freezing calorimeter, we need to use the relation,

$$m_v = 100 \times \rho_s W \tag{18}$$

where m_v is volumetric liquid water expressed in *percent*, and ρ_s is the density of the snow. In our tests, we have converted the freezing calorimeter results to *volume* fractions using the gravimetrically determined density and (18).

3.2.1 Liquid Water Content

The results for the liquid water content comparison are shown in Figure 7. The error bars associated with the freezing calorimeter data points show the range of results obtained from typically two separate (and usually simultaneous) determinations. (Data points with no error bars indicate only a single measurement or that only the mean value of a set was available.) The freezing calorimeter is seen to have generally excellent precision.

The values for m_v obtained from the snow-probe dielectric measurements are computed using equation (13). The data points and error bars shown for the snow probe are based on an average of twelve separate measurements made for each snow sample and the uncertainty of the estimate of the mean

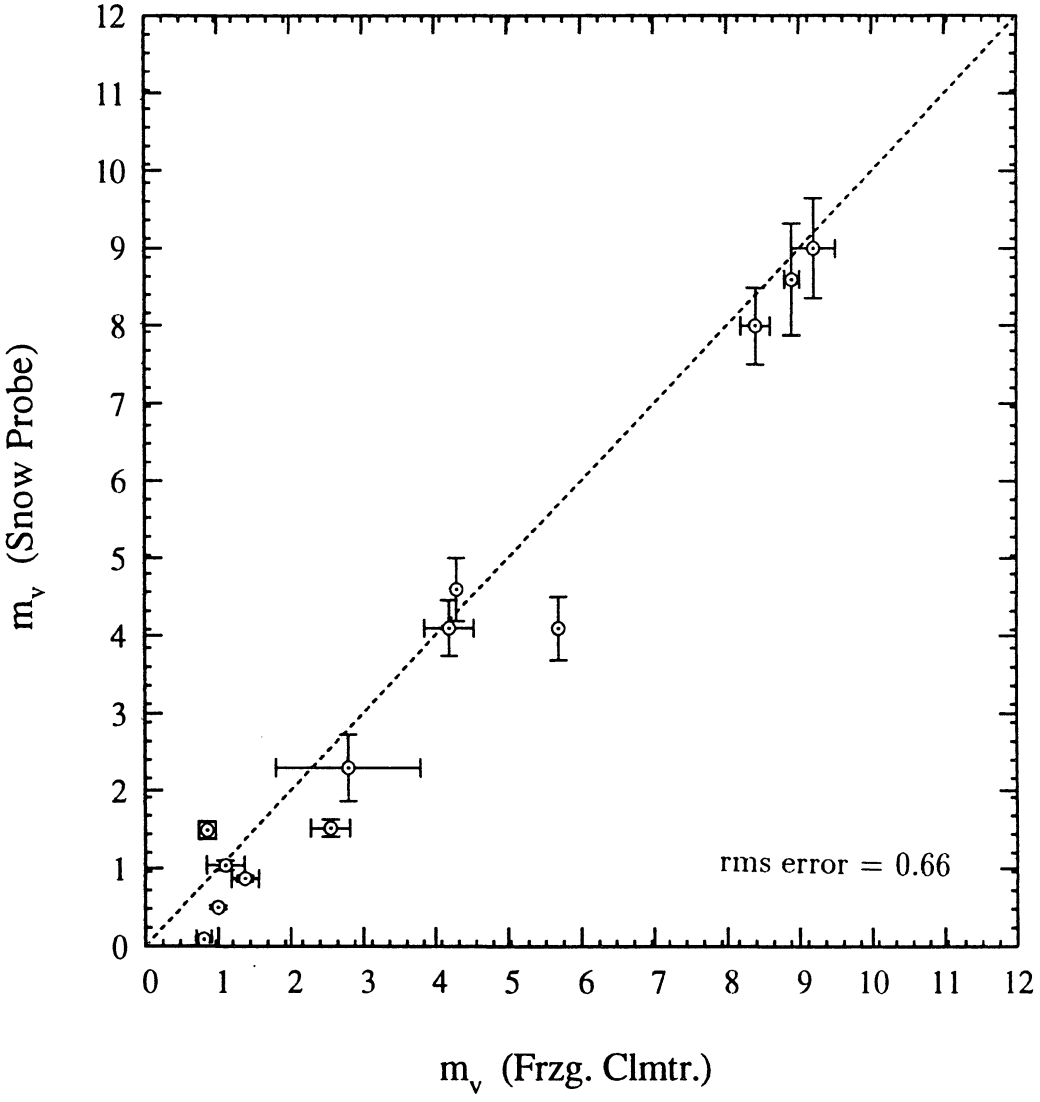

Figure 7: Comparison of snow wetness results obtained *via* snow probe (marks) and freezing calorimetry respectively. Snow probe data points are based on an average of twelve separate measurements.

value as represented by the error bars was computed as $\pm\sigma/\sqrt{N}$ where σ is the standard deviation of the set of measurements and N is the number of measurements in that set. From the figure, it is seen that the agreement between the two techniques is generally very good and, with the exception of an outlier at the 6% level, the use of the snow probe and (13) give results which are within $\pm 0.5\%$ of the freezing calorimeter results. This result strongly supports the validity of equation (13).

3.2.2 Density

The outputs of equations (12) and (11), with dielectric information supplied by our sensor, were compared with the results of gravimetric density measurements. The comparison was conducted over a density range extending between 0.1 and 0.55 g/cm^3. The results are shown in Figure 8. It is seen that, with the exception of a single outlier, excellent agreement is obtained for the cases where the snow volumetric wetness level was $< 3\%$. In contrast, density estimates made *via* (12) and (11) when snow wetness exceeded 3% departed markedly from the gravimetric measurements.

The procedure for the retrieval of density, outlined in Section 3, employs a conceptual quantity $\Delta\epsilon'_{ws}$ (Eq. (12)), which is defined to be a measure of the increase in the real part of the dielectric constant of snow, relative to that for dry snow, which would occur if some of the air in the snow medium was replaced by liquid water. Application of (12) to measured values of ϵ'_{ws} then allows determination of a theoretical ϵ'_{ds}, from which, using (16), a theoretical dry-snow density, ρ_{ds}, may be determined. Wet-snow density, ρ_{ws}, is then related to ρ_{ds} using (17).

The quantity $\Delta\epsilon'_{ws}$ is a function of both the resonant frequency f_r and m_v. Across the frequency range over which the snow probe operates (≈ 0.9 – 1.7 GHz), ϵ' is approximately constant for both water and ice. Hence, $\Delta\epsilon'_{ws}$ may be examined as a function of m_v alone. This function is plotted in Figure 9. Also included are experimental quantities which were generated by taking the difference between measured values of ϵ'_{ws} (averages of typically twelve independent snow probe measurements) and calculated values of ϵ'_{ds}, determined through the use of (17) and (11). The solid curve drawn through the experimental quantities is seen to diverge from the behavior predicted by (12), for $m_v > 2.5$ %.

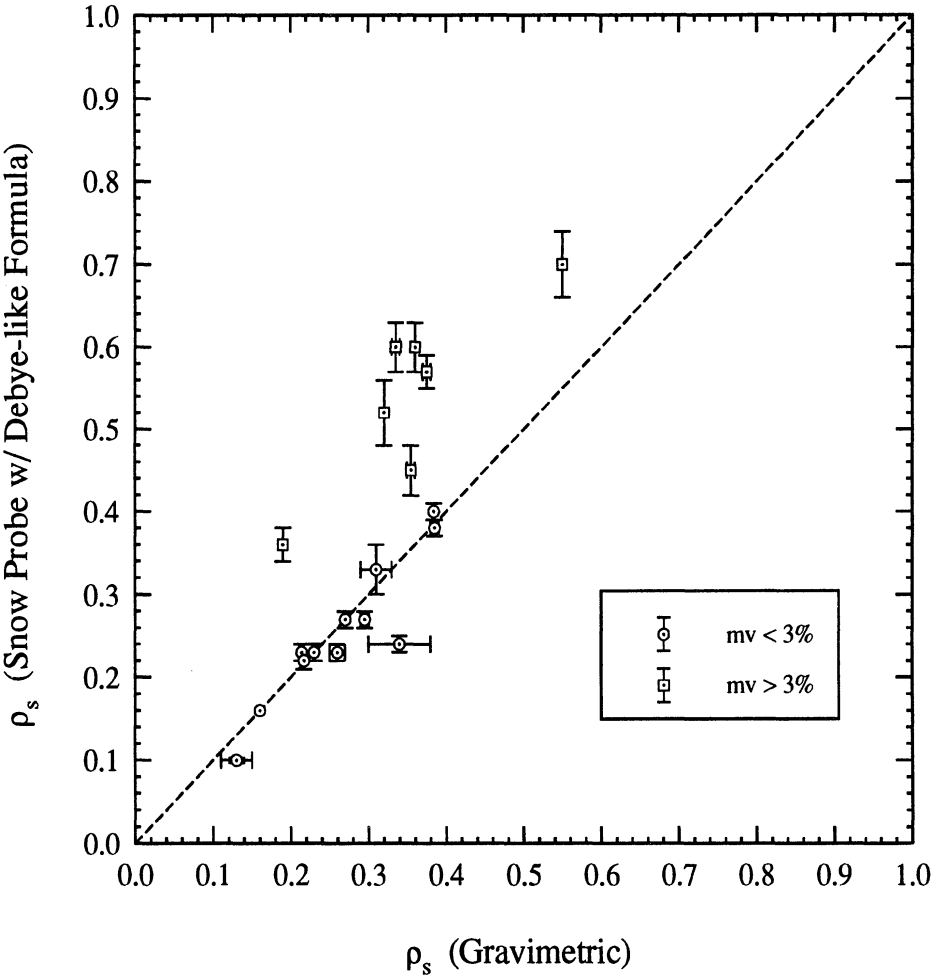

Figure 8: Comparison of snow density results obtained *via* snow probe (with associated relations) and gravimetric measurements. Data points represented with squares were from snowpacks having volumetric wetness levels of $> 3\%$; with circles, $< 3\%$.

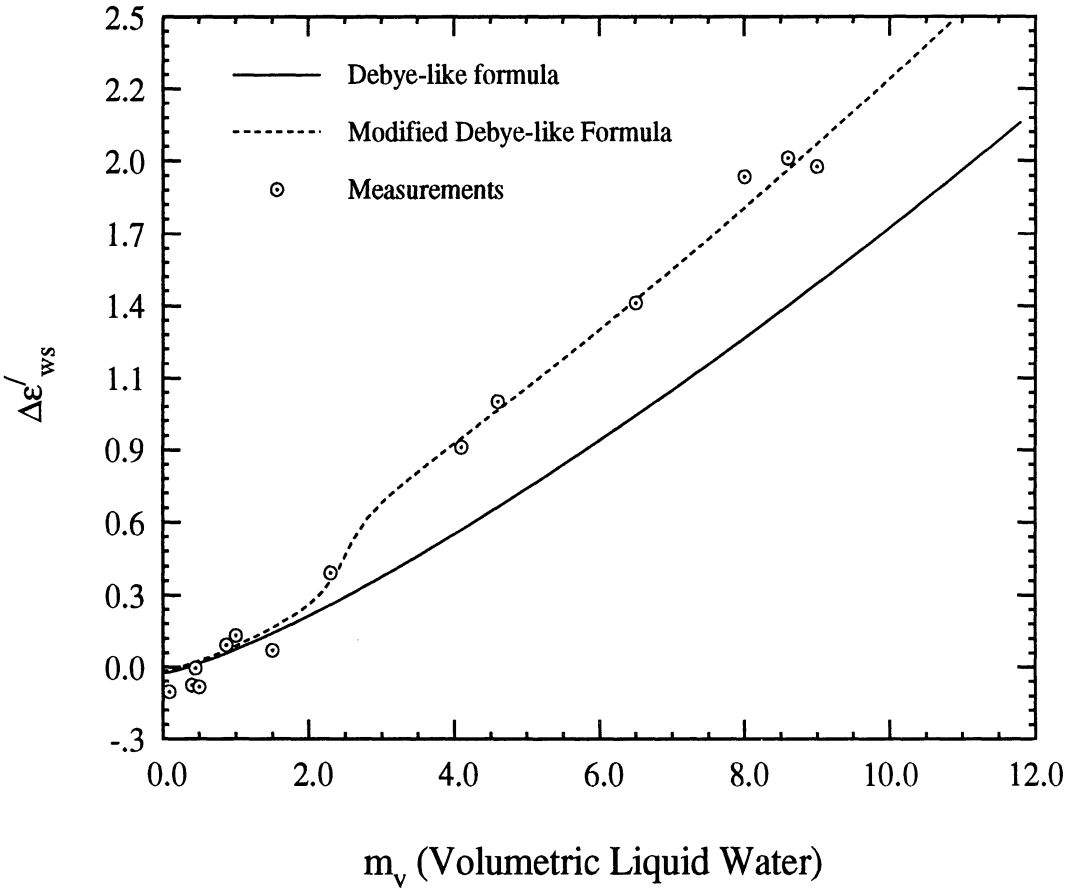

Figure 9: $\Delta\epsilon'_{ws}$ (computed using snow probe-measured ϵ'_{ws}, snow probe-determined m_v, and gravimetrically measured ρ_{ws}) *versus* m_v (snow probe-determined).

This curve is produced by the following function, which is based on the original formula but which is consistant with the observed behavior:

$$\begin{aligned}\Delta\epsilon'_{ws} &= \epsilon'_{ws} - \epsilon'_{ds} \\ &= 0.02 m_v^{1.015} + \frac{0.073 m_v^{1.31}}{1 + (f/f_o)^2} \\ &+ [0.155 + 0.0175(m_v - 2.5)] \left\{ 1 + (2/\pi) \tan^{-1} [4(m_v - 2.5)] \right\}\end{aligned} \tag{19}$$

This function accomodates the essential discontinuity which exists in the data in the neighborhood of $\approx 2.5\%$. Note the data points shown in the figure follow this functional form given in (19) independent of density. As an example, the two data points corresponding to $\approx 4.5\%$ liquid water had densities of 0.19 and 0.55 respectively—yet they still exhibit an incremental $\Delta\epsilon'_{ws}$ according to (19). Having derived (19) from the measured data, we have produced a formula relating measured dielectric constant and snow density which is valid in the region 0.1 to ≈ 0.6 g/cm^3. The sensor data, re-processed using (19) and (11) is compared against the gravimetric data in Figure 10. It is seen that over the range examined, with the exception of one outlier at $\rho \approx 0.34$, the snow probe method agrees with the gravimetric method to within ± 0.03 g/cm^3.

The concept of dry-snow density ρ_{ds}, as understood in the above context, is a conceptual quantity which cannot be measured. Its use is motivated by a desire to attach a physical basis to the dielectric behavior of wet snow; that just as ϵ''_{ws} may be understood in terms of the dispersion behavior of water, so may the behavior of ϵ'_{ws} be understood, as an addition of a quantity based on the dispersion behavior of the real part of the dielectric constant of water, namely equation (12), to ϵ'_{ds}, for which a reliable empirical model exists. The results from the present investigation indicate that the physical reasoning put forth to explain the behavior of ϵ'_{ws} is incomplete; that there are important factors in addition to the real part of the dielectric constant of the water itself.

That there exists, or should exist, an abrupt transition in the dielectric constant of snow as a function of moisture is an idea which has been cited by previous researchers. Colbeck [13] describes a transition between the *pendular* regime, wherein "air occupies continuous paths throughout the pore space"

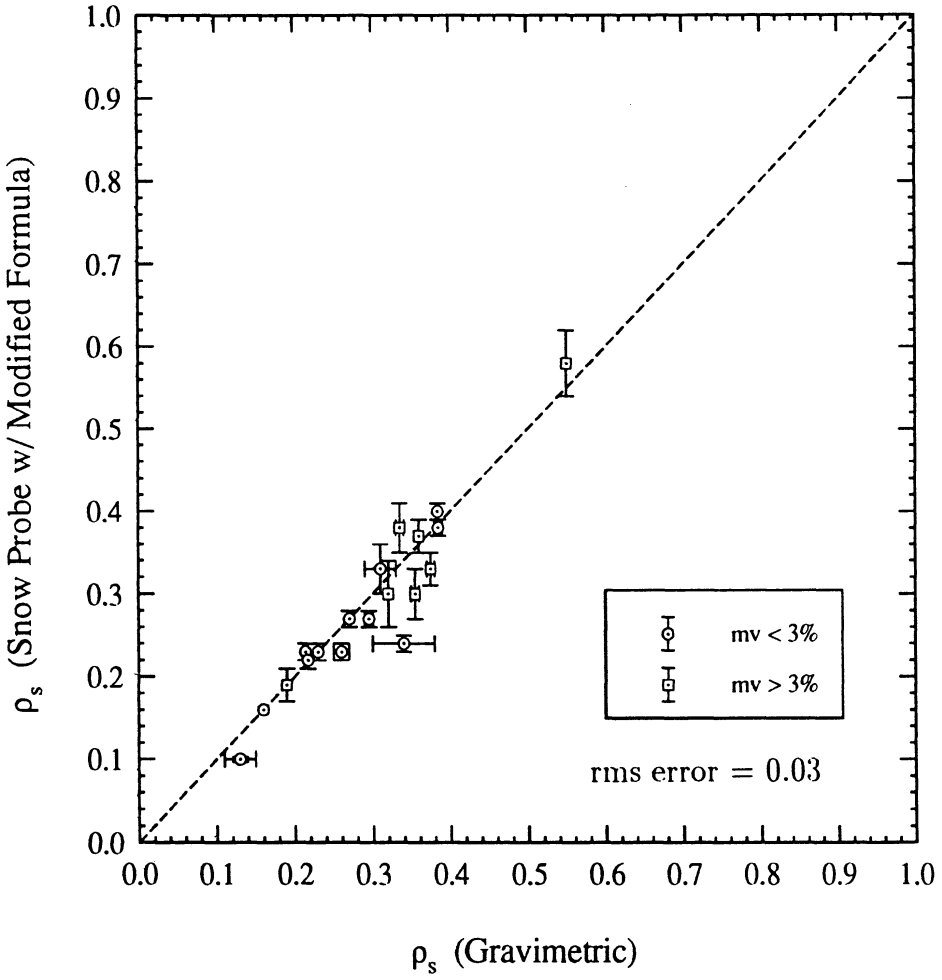

Figure 10: Comparison of snow density results obtained *via* snow probe (with associated *modified* relations) and gravimetric measurements. Data points represented with squares were from snowpacks having volumetric wetness levels of $> 3\%$; with circles, $< 3\%$.

and the *funicular* regime, wherein liquid water "occupies continuous paths throughout the pore space". Denoth [14] estimated this transition at 11 to 15% of the pore volume, which would correspond to 7 to 10% of the total volume for an average snow sample have density 0.3 g/cm^3.

Another description, attributed to Colbeck by Hallikainen *et al.* [2], suggests that such a transition occurs when liquid water inclusions in snow transform from being primarily needle-shaped (at low values of liquid water content) to being primarily disk shaped. In [2], snow dielectric constant data in the 3 to 37 GHz range was analyzed using Polder Van Santen mixing models. It was concluded that the shape factors in the models which provided the best fit to the data supported the concept of a needle-to-disk transformation of the water inclusions. The two-phase Polder Van Santen model with the shape factors (or depolarization coefficients) specified in [2] was applied to the current snow probe data. It was found however to give a result very comparable to the Debye-like model (Equ. 12), that is, it predicts no transition.

4 Conclusion

This report has described the development and validation of an electromagnetic sensor and associated algorithm for the purpose of rapid ($\approx$ 20 seconds) and non-destructive determination of snow liquid water content and density. The sensor is similar in principle to an existing device known as a "Snowfork", but offers additional advantages in spatial resolution and accuracy owing to a novel coaxial-cavity design.

Direct methods of snow wetness determination were evaluated for their suitability as standards against which the device could be tested. The dilatometer, though simple in principle, was found to give very unfavorable performance. The freezing calorimeter, which has, as a system, been brought to a high degree of sophistication in our lab, was found capable of delivering accuracy better than $\pm 1\%$, and excellent precision.

The snow probe determines the dielectric constant directly. Empirical and semi-empirical models use this information to compute liquid water volume fraction and density. To test the suitability of these models, the snow probe was tested against the freezing calorimeter and gravimetric density determinations. In general, excellent agreement was obtained: liquid water

measurement accuracy ± 0.66 % in the wetness range from 0 to 10% by volume; wet snow density measurement accuracy ± 0.03 g/cm^3 in the density range from 0.1 to 0.6 g/cm^3. The relations employed to translate measured dielectric constant to snow parameters were those set forth by Hallikainen [2]. The equation relating ϵ''_{ws} to m_v and frequency was found to be entirely valid. However, the equation predicting $\Delta\epsilon'_{ws}$ in terms of m_v and frequency failed to taken into account an abrupt increase in ϵ'_{ws} which occurs in the range of m_v equal to 2.5 to 3%. This failure results in very large errors in the estimate of density. The formula was accordingly modified (equation (19) to correctly model the observed effect.

Figure 11 is a nomogram, based on these equations which have been found to be valid in the specified ranges. It consists of contours of constant m_v and ρ_{ds} respectively, in a 2-dimensional representation bounded by the two parameters which are directly obtained by the snow probe: resonant frequency and bandwidth (3-dB) of the resonance spectrum. With the measurement of these two quantities, m_v and ρ_{ds} may be uniquely specified. Dry-snow density, ρ_{ds}, is related thru (17) to wet-snow density ρ_{ws}.

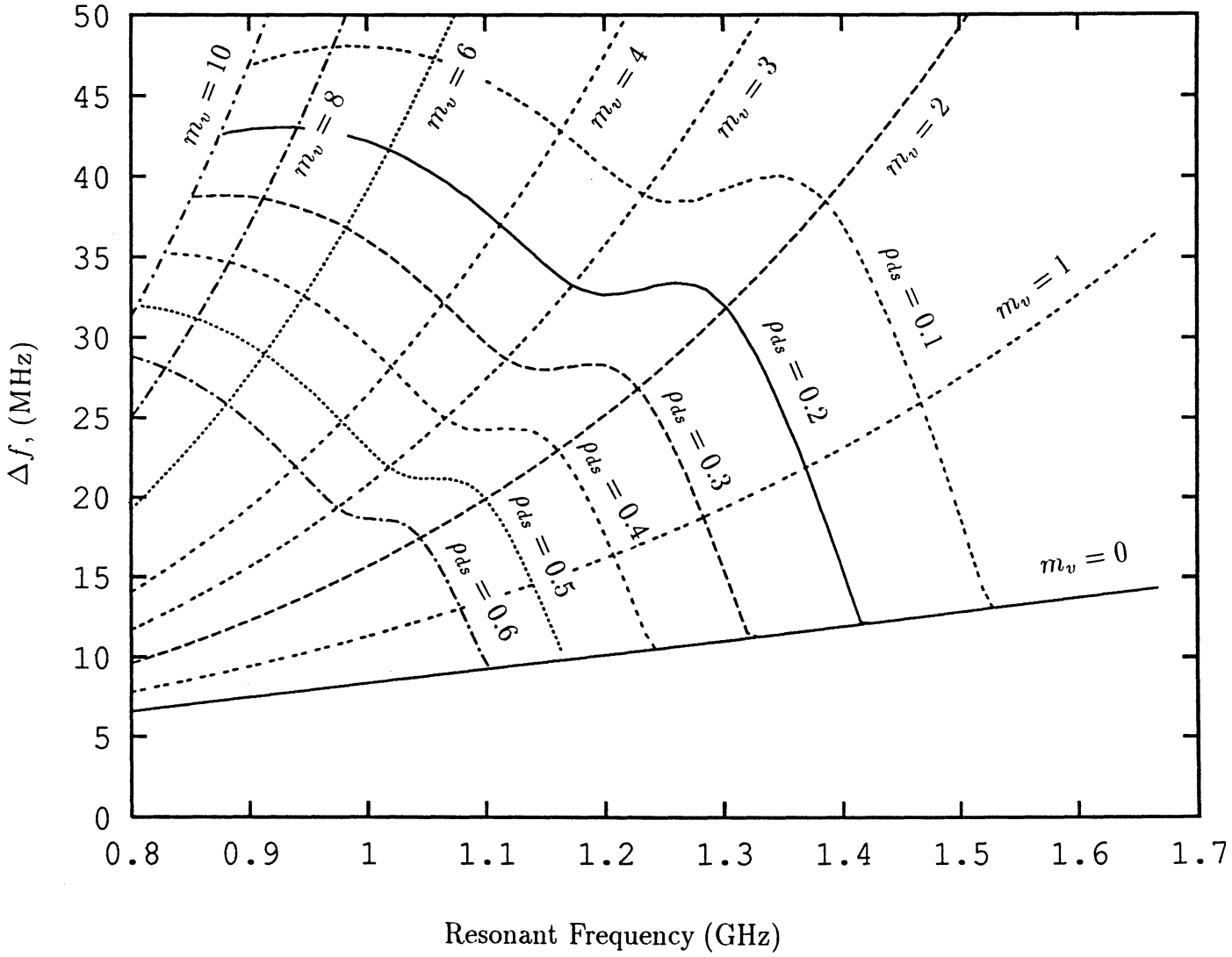

Figure 11: Nomogram giving snow liquid water content (m_v) and equivalent dry-snow density (ρ_{ds}) in terms of two parameters directly measured by the snow probe: resonance frequency (f) and resonance (3-dB) bandwidth (Δf).

References

[1] Sihvola, A., M. Tiuri, "Snow Fork for Field Determination of the Density and Wetness Profiles of a Snow Pack", *IEEE Trans. Geosci. Remote Sensing,* vol. Ge–24, pp. 717–721, 1986.

[2] Hallikainen, M., F. T. Ulaby, M. Abdelrazik, "Dielectric Properties of Snow in the 3 to 37 GHz Range", *IEEE Trans. Antennas Propagat.,* vol. AP–34, pp. 1329–1339, 1986.

[3] Jones, E. B., A. Rango, S. M. Howell, "Snowpack Liquid Water Determinations Using Freezing Calorimetry", *Nordic Hydrol.,* 14, pp. 113–126, 1983.

[4] Tiuri, M. E., A. H. Sihvola, E. G. Nyfors, and M. T. Hallikainen,"The Complex Dielectric Constant of Snow at Microwave Frequencies",*IEEE J. Oceanic Engr.,* vol. OE-9, pp. 377–382, 1984

[5] Stiles, W. H., F. T. Ulaby, *Microwave Remote Sensing of Snowpacks,* NASA Contractor Report 3263, June 1980.

[6] Austin, R. T., *Determination of the Liquid Water Content of Snow by Freezing Calorimetry,* Univ. of Michigan Radiation Lab Report 022872–2, Jan. 1990.

[7] Ellerbruch, D. A., and H. S. Boyne, "Snow Stratigraphy and Water Equivalence Measured with an Active Microwave System", *J. Glaciol.,* vol. 26, pp. 225–233, 1980.

[8] Colbeck, S. C., "The Layered Character of Snow Covers", *Revs. of Geophys.,* 29, pp. 81–96, 1991.

[9] Collin, R. E., *Foundations for Microwave Engineering,* New York: McGraw-Hill, 1966.

[10] Nyfors, E. and Vainikainen, P., *Industrial Microwave Sensors,* Norwood, MA: Artech House, 1989.

[11] Altschuler, H. M., "Dielectric Constant", *Handbook of Microwave Measurements,* vol. II, 3rd ed., Polytechnic Press, 1963.

[12] Leino, M. A. H., P. Pihkala, and E. Spring, "A Device for Practical Determination of the Free Water Content of Snow", *Acta Polytechnica Scandinavica,* Applied Physics Series No. 135, 1982.

[13] Colbeck, S.C, "An Overview of Seasonal Snow Metamorphism", *Rev. Geophys. Space Phys,* vol. 20, pp. 45–61, 1982.

[14] Denoth, A., "The Pendular-Funicular Transition in Snow", *J. Glaciol.,* 25(91), pp. 93–97, 1980

APPENDIX A: Evaluation of Dilatometer and Freezing Calorimeter

A.1 Dilatometer Evaluation

Attracted by the simplicity of the concept, apparatus, and procedure, we expended considerable effort in evaluating the dilatometer technique. As we ultimately rejected it as a result of its poor performance in determining liquid water content, we will not go into the details of the apparatus itself; a complete description is provided in [12] for those interested. Instead, we will just briefly describe the method and then present some of the drawbacks that led us to reject the method.

In the method, a weighed snow sample is placed in a cooled (0°C) jar, and then the jar is completely filled with 0°C water. A lid with a graduated tube is fixed onto the jar, and the tube itself is filled with freezing water and the level noted. The jar is placed in a warm water bath to melt the snow and then the entire system is returned to a temperature very close to 0°C. The change in the volume is related to the mass of ice present, and subtracting this from the original snow mass gives the mass of water in the snow sample.

The principal drawbacks we found were the following:

- Lack of accuracy due to non-ideal behavior of the materials. We tried the following experiment: we filled the apparatus entirely up with 0°C water (no snow or ice) and cycled the temperature up and then back down as described above. In each of several trials, the volume of the water (which should have returned to its original value, about 1 liter) was found to have increased by about 0.1%, enough to cause a very significant error in an actual trial. In quantitative terms, if a 75 gram sample of snow having 5% water mass fraction was analyzed, it would appear that the sample had 20% water mass fraction. We believe this volume expansion effect may be caused by gases that are liberated when the cold water is warmed. Additional slight but critical volume changes may be caused by expansion or contraction of any of the parts of the dilatometer apparatus.

- Long analysis time. The snow, once added, can be melted relatively quickly by warming the system. However, to return back to 0°C (which

is absolutely critical to avoid unwanted volume changes in the system) the wait required is on the order of one hour. The reason is that, unlike the warming case, for the cooling there is a relatively small temperature gradient. The bath can be no less then 0°C; so when the temperature gets down to 5 or 6°C, there is very little gradient to drive it down further.

A.2 Freezing Calorimeter Evaluation

As noted earlier, the theoretical background and the procedural details of the freezing calorimeter method are thoroughly discussed in a previous Radiation Lab report [6]. Since that report was written, there have been several major improvements made in the freezing calorimeter system:

- A second calorimeter was constructed, identical to the first, to allow for duplicate measurements to be done in parallel.
- A motorized tripod-mounted mechanical shaker was constructed which is capable of shaking both calorimeters simultaneously.
- The system has been made PC–based. Software was written which handles two calorimeter channels independent of one another. Data from each channel is collected, displayed, and reduced automatically by the computer.

The method, with these improvements, was tested for precision and accuracy. To our knowledge, it is the first time a systematic test of the method precision and accuracy has been performed.

The accuracy of the method was tested at three different levels of wetness. We prepared a sample of snow with zero wetness by placing it in a freezer at −20°C for several hours. Four separated analyses were performed on the snow from this batch. To test at two other wetness levels, at the point in the procedure where the lid is removed from the calorimeter and snow added, we added—in addition to the zero-wetness snow from above—a precisely measured volume of water at exactly 0°C. In this way, we "spiked" dry snow samples at levels corresponding to 5% and 11% liquid water mass fraction. Each case was analyzed in duplicate. The results of the accuracy tests performed at these three levels are shown in Figure A.1. Shown is

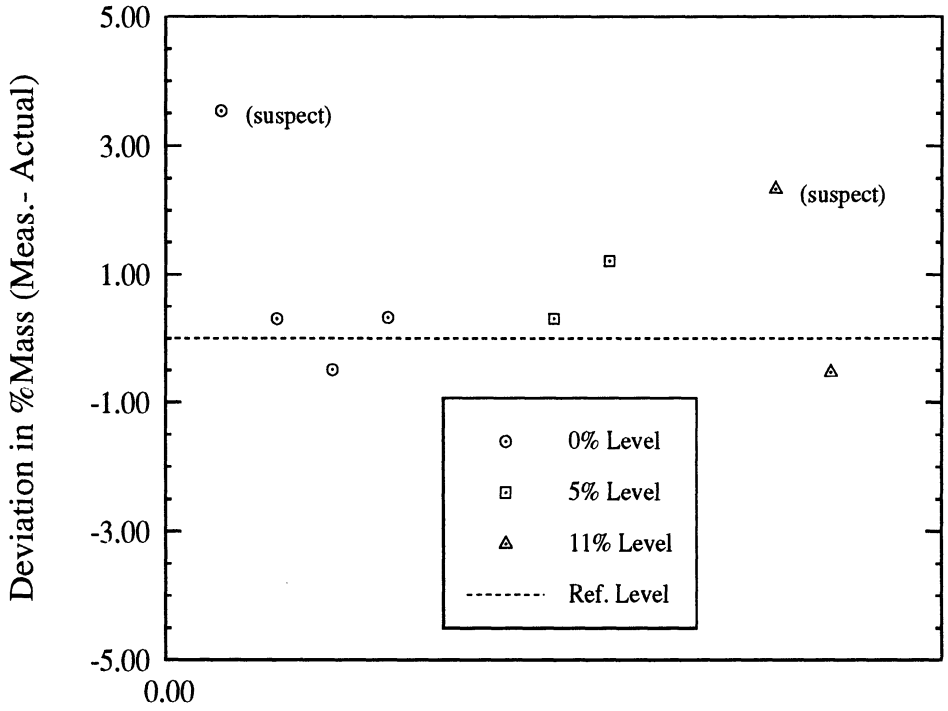

Figure A.1: Calorimeter accuracy tested at three different levels of water content. Data is normalized so all results are compared to what actual level was calculated to be in each case. The two points marked "suspect" correspond to analyses noted at the time of execution as problematic.

the degree to which the experimental results deviated from the known mass fractions. Two results, one at the 0% level and one at the 11% level, come from analyses which were noted as problematic at the time of analysis, and are marked as "suspect". From these tests, it appears that the method is accurate to a level somewhat better than $\pm 1\%$.

The precision of the method was clearly observed since all analyses were done in duplicate. From the results shown in Figure A.1 and the results which will be seen in the next section wherein the calorimeter is compared to the snow probe, it seems that the precision is on the order of $\pm 0.5\%$.

APPENDIX B: Resonant Cavity Measurements of Dielectric Constant

The L-band cavity used for the present study was a cylindrical, transmission-type resonator, with diameter 13.9 cm and depth 6.35 cm. The TM_{010} mode is resonant at 1.64618 GHz and the loaded (measured) Q for the air-filled cavity was $\approx$ 3750. To insure reliable, reproducible performance, the cover of the resonator was always fixed on using a torque wrench (60 ft-lbs) and following a prescribed pattern in tightening the screws.

In the most general case, the quality factor of a resonant system is given as follows:

$$\frac{1}{Q_l} = \frac{1}{Q_u} + \frac{1}{Q_{ext}} \tag{B.1}$$

where, Q_l is the *loaded* Q, Q_u is the *unloaded* Q, and Q_{ext} the *external* Q. The unloaded Q is the "real" Q of the resonator but it is possible to measure it directly. The coupling devices (loops, probes) used to couple power in and out of the resonator also contribute to power leakage out (represented by Q_{ext}) which is a source of loss not inherently related to the resonator itself or its contents. The reciprocal of Q_u may be written as the sum:

$$\frac{1}{Q_u} = \frac{1}{Q_R} + \frac{1}{Q_d} + \frac{1}{Q_m} \tag{B.2}$$

where Q_R is, as before, related to the radiated losses, Q_d to the dielectric losses, and Q_m to the losses associated with the metal walls of the resonator having a finite conductivity. For a closed resonator, as ours is, the radiated losses are zero and we need not consider Q_R. Also, for the empty (air-filled) resonator, Q_d is not considered. Furthermore, it can be demonstrated [10] that for a resonator filled with a dielectric ϵ,

$$\frac{1}{Q_m} = \frac{\sqrt[4]{\epsilon}}{Q_{mo}} \tag{B.3}$$

where Q_m is associated with the metal losses in the dielectric-filled cavity, and Q_{mo} with the metal losses in the air-filled cavity. From (5) the loss tangent $\tan\delta$ may be found from Q_d which may in turn be obtained if Q_u as given in (B.2) may be found and (B.3) is also used. The problem then becomes how,

upon measuring Q_l (see equation (B.1)), may Q_u be determined? For the most general case of the input and output coupling networks being different, Altschuler ([11]) describes a general impedance method for determining Q_u from Q_l. If it is assumed that the input and output coupling networks are equivalent, then Q_u can be directly calculated [10] from measurements of Q_l and the insertion loss a_r at the resonant frequency as follows:

$$Q_u = \frac{Q_l}{1 - \sqrt{a_r}} . \tag{B.4}$$

For our L-band cavity, it was found that the simple method above gave very comparable results to the general impedance method in all cases. It is noted that the general impedance method detailed in [11] is considerably more involved than that given by (B.4).

Based on the above discussion, the procedure for determining dielectric constants with a resonant cavity is summarized as follows:

- Real part of dielectric is found in the same way as given in equation (1), using the resonant frequencies of the dielectric-filled and air-filled cavity.

- Imaginary part of dielectric requires determination of Q_u. Then for the case of equivalent input and output coupling factors, equations (5),(B.3), and (B.4) lead to,

$$\epsilon'' = \epsilon' \left\{ \frac{1}{Q_l} [1 - \sqrt{a_r}\,] - \frac{\sqrt[4]{\epsilon'}}{Q_{mo}} \right\} \tag{B.5}$$

  where

$$\frac{1}{Q_{mo}} = \frac{1}{Q_{lo}} [1 - \sqrt{a_{ro}}\,] = \frac{1}{Q_{lo}} - \frac{1}{Q_{ext,o}} \tag{B.6}$$

  where the "o" in the subscripts refers to quantities associated with the air-filled cavity.

APPENDIX C: Snow Probe Program Listing

This appendix contains the computer program used in conjunction with the snow probe. It is written in HP Basic. See Section 3.4 for additional details of the snow probe system.

```
************************************************************************
2     ! Program SNOWFORKB !
3   OPTION BASE 1
4   COM /Flag/ Qflag,Cal_flag
5   COM /Values/ Fstart,Pwrl,Det_max
6   COM /Addr/ @Swp,@Dvm
7   COM /Cal_vals/ Mslope,B_cept,F_air
8   COM /File_info/ F_flag,Stars$[15],F_name$[12],@Path1,Dumm
9   COM /Line_loss/ Pstep,Pfrac,Pflag
10  MASS STORAGE IS "SNOWFORK/:CS80, 700, 0"
12  INITIALIZE ":,0",9      !CREATE MEMORY VOLUME TO HOLD FILE.
13  STORE KEY "KEY_DEFS:,0"    !STORE KEY DEFN'S IN FILE "KEY_DEFS"
14  DIM A$(23)[1]      !
15  SET KEY 0,A$(*)     !REDEFINE ALL KEYS TO UNDEFINED.
16  CLEAR SCREEN
17  ON KEY 0 LABEL "TAKEDATA" CALL Takedata
18  ON KEY 1 LABEL "CALIBRATE" CALL Calibrate
19  ON KEY 9 LABEL "QUIT" CALL Quit
20  ON KEY 3 LABEL "CREATE_FILE" CALL Create_file
21  ON KEY 4 LABEL "CLOSE_FILE" CALL Close_file
22  ON KEY 5 LABEL "PWR_LVL" CALL Pwr_lvl
23  ON KEY 6 LABEL "START_FREQ" CALL Start_freq
24  !ON KEY 8 LABEL "SAMPLE_RATE" CALL Rate
26   !ON KEY 8 LABEL "CAL_LINE_LOSS" CALL Cal_line
27  KEY LABELS ON
28  ON ERROR RECOVER Getfree
30  PLOTTER IS CRT,"INTERNAL"
31  Pflag=0
32  Pstep=2.09*.01
33  Dumm=10
34  Fstart=.95
35  Pwrl=0
36  Mslope=4.53
37  B_cept=5.36
38  F_air=1.663
39  PRINT "CURRENTLY, Mslope = ";Mslope;"  B_cept = ";B_cept
40  PRINT "AND,  F_air = ";F_air
41  F_flag=0      ! Denotes no file opened yet.
42  Cal_flag=0     ! Denotes Cal not in progress.
43  Stars$="***************"     ! Dividers between file entries.
44  Qflag=0
```

```
45 Choose:  !
46  INPUT "WHICH DETECTOR (1,2,OR 3)?",Detect
47  SELECT Detect
48  CASE 1
49     Det_max=.00500
50  CASE 2
51     Det_max=.00089
52  CASE 3
53     Det_max=.00056
54  CASE ELSE
55     BEEP
56     PRINT "INVALID CHOICE"
57     GOTO Choose
58  END SELECT
59  ASSIGN @Dvm TO 702
60  ASSIGN @Swp TO 719
61  OUTPUT @Swp;"IP"
63  WHILE Qflag<>1
64  END WHILE
65  LOAD KEY "KEY_DEFS:,0"     ! RELOAD OLD KEY DEFN'S.
66  INITIALIZE ":,0",0      ! RECLAIM MEMORY VOLUME STORAGE.
67 Getfree:  !
68 IF F_flag=1 THEN ASSIGN @Path1 TO *
69 PRINT "Program Exited"
70  END
71   !
72   !
73  SUB Takedata
74     REAL B(1:250)
75     DIM Comment$[200]
76     COM /Line_loss/ Pstep,Pfrac,Pflag
77     COM /Addr/ @Swp,@Dvm
78     COM /Values/ Fstart,Pwrl,Det_max
79     COM /Results/ E1,E11,F0,Q,Mv,Pws
80     COM /Cal_vals/ Mslope,B_cept,F_air
81     COM /File_info/ F_flag,Stars$,F_name$,@Path1,Dumm
82     COM /Flag/ Qflag,Cal_flag
83     COM /Samp_rate/ Srate$[2]
84     Comment$="
85     IF Cal_flag=1 THEN GOTO Jump1
86     IF F_flag=1 THEN
87        PRINT "Current comment is:"
88        PRINT Comment$
89        INPUT "Enter comment or description if desired:",Comment$
90        PRINT "Press continue to take data:"
91        PAUSE
92     END IF
93 Jump1:        !
94     GINIT
95     GRAPHICS ON
96     GCLEAR
97     CLEAR SCREEN
98     N=80
99     FOR I=1 TO 250
100       B(I)=0
```

```
101    NEXT I
102      !Pstep=INT(.209*.01/.006)*.006
103      !INPUT "ENTER POWER STEP:",Pstep
104    Pstep=.067
105    OUTPUT @Swp;"PL";Pwrl;"DM CW";Fstart;"GZ SF10MZ"
106  ! Instrument preset: power 0 dBm,start @ fstart GHz,
107  ! step size = 10 MHz.
109   !  OUTPUT @Dvm;"T1 F1 R-2 N3 Z0 D3"!Int. trig., DC volts,
110      ! 30 mV DC, 3.5 digits, autozero off, display off.
111      !
112      ! DIFFERENT CMD FOR FLUKE 8842A METER:
113    OUTPUT @Dvm;"* T0 F1 R8 S2 D0" !Int. trig., DC volts,
114      ! 20mV DC, fast aqu., display off.
115      !
116    VIEWPORT 10,120,25,75
117    FRAME
118     !WINDOW 1,84,-9.E-3,1.2E-2
119    WINDOW 1,84,-.5*Det_max,1.5*Det_max
120    FOR I=1 TO 84
121       ENTER @Dvm;Dum
122       B(I)=-Dum
123          !OUTPUT @Swp;"PL UP CW UP"
124       OUTPUT @Swp;"UP"
125       PLOT I,B(I)
126    !PRINT B(I)
127    NEXT I
128    Bmax=MAX(B(*))
129   !PRINT "Max value:",Bmax
130    !GOTO Jump3
131      !
134    Delt=B(84)/Bmax   !FRACTION OF ATTN.
135    Fdelt=.84      !gHZ
136    Pfrac=Delt/Fdelt
137    IF Pflag=1 THEN
138       SUBEXIT
139    END IF
140    K=1
141    WHILE B(K)<>Bmax
142       K=K+1
143    END WHILE
144    Freq=Fstart+(K-1)*.010
145    F1=Freq-.06
146    Ss=.120/N
147      !Pstep2=Pstep*.0015/.01
148    OUTPUT @Swp;"PL";Pwrl;"DM CW";F1;"GZ SF";Ss;"GZ"
149      !
150    FOR I=1 TO 250
151       B(I)=0
153    NEXT I
154  ! OUTPUT @Dvm;Srate$
155   FOR I=1 TO N/2
156      ENTER @Dvm;Dum
157    ! B(I)=-Dum+(I-1)*.001*1.117E-2
158      B(I)=-Dum
159      OUTPUT @Swp;"UP"
```

```
160     OUTPUT @Swp;"UP"
161   NEXT I
162      !
163      !
164    Bmax=MAX(B(*))
165      ! Adjust power level for optimum snr:
166      !
167 ! P_level=10^((Pwrl)/10)
168 P_level=10^((Pwrl-10)/10)
169  Pwrl=P_level*(Det_max/Bmax)
170  Pwrl=10*LGT(Pwrl)
171  Pwrl=INT(Pwrl/.004)*.004+10
172  OUTPUT @Swp;"pl";Pwrl;"DM CW";F1;"GZ"
173  ! OUTPUT @Dvm;Srate$
174   FOR I=1 TO N
175      ENTER @Dvm;Dum
176      !B(I)=-DUM+(I-1)*.001*1.117E-2
177      B(I)=-Dum
178      OUTPUT @Swp;"UP"
179   NEXT I
180   Pwrl=3
182   OUTPUT @Swp;"PL";Pwrl;"DM"
184   Bmax=MAX(B(*))
185    Half=Bmax/2
186    K=1
187    Btest=B(1)
188    IF (Btest>Half) THEN
189       PRINT "Leading edge of peak not in bracketed region."
190       PRINT "Press Continue to proceed."
191       PAUSE
192       CLEAR SCREEN
193       GCLEAR
194       GOTO Jump3
195    END IF
196    WHILE Btest<Half
197       K=K+1
198       Btest=B(K)
199    END WHILE
200    IF Btest=Half THEN
201       F3db=F1+(K-1)*Ss
202    ELSE
203       Delts=(Half-B(K-1))/(B(K)-B(K-1))
204       F3db=F1+(K-2+Delts)*Ss
205    END IF
206    Khalf=(F3db-F1)/Ss
207    WHILE B(K)<>Bmax
208       K=K+1
209    END WHILE
210    !
211    ! Find out if there are duplicate max pts., if so, choose
212    ! center one.
213    !
214    K1=K
215    WHILE B(K1)=Bmax
216    K1=K1+1
```

```
217    END WHILE
218    K=INT((K+K1)/2)
219    F0=F1+(K-1)*Ss
220    Kk=K
221    Btest2=B(Kk)
222    WHILE Btest2>Half
223       Kk=Kk+1
224       Btest2=B(Kk)
225       IF (Kk=N+1) THEN
226          PRINT "Trailing edge of peak not in bracketed region."
227          PRINT "Press Continue to proceed."
228          PAUSE
229          CLEAR SCREEN
230          GCLEAR
231          GOTO Jump3
232       END IF
233    END WHILE
234    IF Btest2=Half THEN
235       F3db2=F1+(Kk-1)*Ss
236    ELSE
237       Delts=(Half-B(Kk-1))/(B(Kk)-B(Kk-1))
238       F3db2=F1+(Kk-2+Delts)*Ss
239    END IF
240    Khalf=(F3db-F1)/Ss
241    Khalf=Khalf+1
242    Khalf2=(F3db2-F1)/Ss
243    Khalf2=Khalf2+1
244      ! COMPUTE Q:
245    Fdelt=ABS(F3db-F3db2)
246    Q=F0/Fdelt
247      !
248      ! CALCULATE COMPLEX DIELECTRIC CONSTANT,
249      ! AND COMPUTE SNOW MOISTURE AND DENSITY.
250      !
251    E1=(F_air/F0)^2
252    Bw=Mslope*F0+B_cept
253    E11=E1*((1/Q)-Bw/(F0*1000))
254    IF E11<0 THEN E11=0
255      !
256      ! COMPUTE LIQUID WATER VOL. FRAC & DENSITY.
257      !
258    A1=F0/9.07
259    Mv=(E11*(1+A1^2)/(.075*A1))^(1./1.31)
260    Eds=E1-.02*Mv^1.015-.073*Mv^1.31/(1+A1^2)
261    Neweds=E1-.25*SQRT(Mv)-.25*(A1)*Mv^1.8/(1+A1^2)
262    Newpds=-1.214+(1.474-1.428*(1-Neweds))^(1/2)
263    Newpws=Mv/100+Newpds
264    Pds=-1.214+(1.474-1.428*(1-Eds))^(1/2)
265    Pws=Mv/100+Pds
266    GCLEAR
267    VIEWPORT 10,120,25,75
268    FRAME
269    WINDOW 1,N,0,1.1*Bmax
270    FOR I=1 TO N
271       PLOT I,B(I)
```

```
272    NEXT I
273    LORG 5
274    MOVE K,Bmax
275    LABEL "+"
276    MOVE Khalf,Half
277    LABEL "x"
278    MOVE Khalf2,Half
279    LABEL "x"
280    PRINT "Center Freq. = :",F0
281    PRINT "Q = :",Q
282    PRINT "Dielectric Constant:",E1,"-j",E11
283    PRINT "mv = :",Mv
284    PRINT "Wet snow density = :",Pws,"      Bmax = ",Bmax
285    PRINT "OR (revised) density = :",Newpws
286    MOVE 0,-Bmax
287    IF Cal_flag=1 THEN GOTO Jump3
288    IF F_flag=1 THEN
289       INPUT "Store this data (Y/N)?",Answ$
290       IF (Answ$="Y" OR Answ$="y") THEN
291          CLEAR SCREEN
292          GCLEAR
293          OUTPUT @Path1;FNPr$(Dumm+1)&TIME$(TIMEDATE)
294          OUTPUT @Path1;FNPr$(Dumm+2)&"Comment: "&Comment$
295          OUTPUT @Path1;FNPr$(Dumm+3)&"Res. Freq.: "&VAL$(F0)
296          OUTPUT @Path1;FNPr$(Dumm+4)&"Q: "&VAL$(Q)
297          OUTPUT @Path1;FNPr$(Dumm+5)&"Dielectric const.:"&VAL$(E1)&"
                    - j"&VAL$(E11)
298          OUTPUT @Path1;FNPr$(Dumm+6)&"mv : "&VAL$(Mv)
299          OUTPUT @Path1;FNPr$(Dumm+7)&"Wet density: "&VAL$(Pws)
                   &"(REVISED)"&VAL$(Newpws)
300          OUTPUT @Path1;FNPr$(Dumm+8)&"DET_MAX: "&VAL$(Det_max)&"
                    and B_max = "&VAL$(Bmax)
301          OUTPUT @Path1;FNPr$(Dumm+9)&Stars$
302          Dumm=Dumm+9
303       END IF
304    END IF
305 Jump3:
306 SUBEND
307       !
308       !
309 SUB Quit
310    COM /Flag/ Qflag,Cal_flag
311    Qflag=1
312    GCLEAR
313 SUBEND
314       !
315       !
316 SUB Calibrate
317    COM /Avgs/ Fs,Qs,Fa,Qa,Caltype
318    COM /Cal_vals/ Mslope,B_cept,F_air
319    COM /Flag/ Qflag,Cal_flag
320    COM /File_info/ F_flag,Stars$,F_name$,@Path1,Dumm
321    PRINT "May read in most recent cal parameters or re-calibrate."
322    INPUT "Do you wish you read in old values (y/n)?",Answ$
323    IF (Answ$="y" OR Answ$="Y") THEN
```

```
324       ASSIGN @Path_2 TO "CALVALS"
325       ENTER @Path_2;Mslope,B_cept,F_air
326       ASSIGN @Path_2 TO *
327       PRINT "New values of mslope,b_cept, and f_air are:"
328       PRINT Mslope,B_cept,F_air
329    END IF
330    OFF KEY
331    ON KEY 1 LABEL "HEPTANE",3 CALL Sugar
332    ON KEY 2 LABEL "AIR",3 CALL Air
333    ON KEY 3 LABEL "ESCAPE",3 CALL Quit
334    ON KEY 4 LABEL "COMPUTE",3 CALL Compute
335    WHILE Qflag<>1
336    END WHILE
337      ! RESET QFLAG.
338    Qflag=0
339    IF F_flag=1 THEN
340       INPUT "Store cal data to file (Y/N)?",Answ$
341       IF (Answ$="Y" OR Answ$="y") THEN
342          OUTPUT @Path1;FNPr$(Dumm+1)&TIME$(TIMEDATE)
343          OUTPUT @Path1;FNPr$(Dumm+2)&"HEPTANE: "&VAL$(Fs)&",
               "&VAL$(Qs)
344          OUTPUT @Path1;FNPr$(Dumm+3)&"Air: "&VAL$(Fa)&" ,"&VAL$(Qa)
345          OUTPUT @Path1;FNPr$(Dumm+4)&"BW = "&VAL$(Mslope)&" x f
                 + "&VAL$(B_cept)
346          OUTPUT @Path1;FNPr$(Dumm+5)&Stars$
347          Dumm=Dumm+5
348       END IF
349    END IF
350 SUBEND
351       !
352       !
353 SUB Compute
354    COM /Avgs/ Fs,Qs,Fa,Qa,Caltype
355    COM /Cal_vals/ Mslope,B_cept,F_air
356    Bws=Fs*1000*(1/Qs-8.00E-5/1.925)
357    Bwa=Fa*1000/Qa
358    Mslope=(Bwa-Bws)/(Fa-Fs)
359    F_air=Fa
360    B_cept=Bws-Mslope*Fs
361      !
362      ! STORE CAL VALUES IN FILE FOR RETRIEVAL.
363    PURGE "CALVALS"
364    CREATE BDAT "CALVALS",1
365    ASSIGN @Path_2 TO "CALVALS"
366    OUTPUT @Path_2;Mslope,B_cept,F_air
367    ASSIGN @Path_2 TO *
368    ASSIGN @Path_2 TO "CALVALS"
369      !
370    CLEAR SCREEN
371    GCLEAR
372    PRINT "Bw = ";Mslope;" x f + ";B_cept
373 SUBEND
374       !
375       !
376 SUB Cal_main
```

```
377    COM /Avgs/ Fs,Qs,Fa,Qa,Caltype
378    COM /Cal_arrays/ F(10),Q2(10),N
379    COM /Flag/ Qflag,Cal_flag
380    N=0
381    Fsum=0
382    Qsum=0
383    OFF KEY
384    ON KEY 1 LABEL "GETDATA",5 CALL Getdata
385    ON KEY 2 LABEL "DONE",5 CALL Quit
386    WHILE Qflag<>1
387    END WHILE
388    IF N=0 THEN GOTO Jump
389    FOR I=1 TO N
390       Fsum=Fsum+F(I)
391       Qsum=Qsum+Q2(I)
392    NEXT I
393    IF Caltype=1 THEN
394       Fs=Fsum/N
395       Qs=Qsum/N
396    ELSE
397       Fa=Fsum/N
398       Qa=Qsum/N
399    END IF
400 Jump:       !
401    Qflag=0
402 SUBEND
403       !
404       !
405 SUB Getdata
406    COM /Cal_arrays/ F(*),Q2(*),N
407    COM /Results/ E1,E11,FO,Q,Mv,Pws
408    COM /Flag/ Qflag,Cal_flag
409    Cal_flag=1
410    N=N+1
411    PRINT "Insert snow sensor and hit continue."
412    PAUSE
413    CALL Takedata
414    Cal_flag=0
415    INPUT "Use this one in calibration (Y/N)?",Answ$
416    IF (Answ$<>"Y" AND Answ$<>"y") THEN
417       N=N-1
418    ELSE
419       F(N)=FO
420       Q2(N)=Q
421    END IF
422    CLEAR SCREEN
423    GCLEAR
424    PRINT "VALUES SO FAR..."
425    FOR I=1 TO N
426       PRINT "F = :",F(I),"Q = :",Q2(I)
427    NEXT I
428 SUBEND
429       !
430       !
431 SUB Sugar
```

```
432     COM /Avgs/ Fs,Qs,Fa,Qa,Caltype
433     Caltype=1
434     CALL Cal_main
435  SUBEND
436        !
437        !
438  SUB Air
439     COM /Avgs/ Fs,Qs,Fa,Qa,Caltype
440     Caltype=2
441     CALL Cal_main
442  SUBEND
443   !
444   !
445  SUB Start_freq
446     COM /Values/ Fstart,Pwrl,Det_max
447     CLEAR SCREEN
448     GCLEAR
449     PRINT "PRESENTLY, STARTING FREQ. IS ";Fstart;" GHz."
450     INPUT "ENTER DESIRED STARTING FREQ. IN GHz:",Fstart
451  SUBEND
452   !
453   !
454  SUB Pwr_lvl
455     COM /Values/ Fstart,Pwrl,Det_max
456     CLEAR SCREEN
457     GCLEAR
458     PRINT "PRESENTLY, POWER LEVEL IS ";Pwrl;" dBm."
459     PRINT "ALLOWED RANGE IS 0 TO 15 dBm."
460     INPUT "ENTER DESIRED POWER LEVEL:",Pwrl
461  SUBEND
462   !
463   !
464  SUB Create_file
465     DIM String3$[200]
466     COM /File_info/ F_flag,Stars$,F_name$,@Path1,Dumm
467   !
468     GCLEAR
469     CLEAR SCREEN
470     Str1$=DATE$(TIMEDATE)
471     Str2$=TIME$(TIMEDATE)
472     F_name$=Str1$[1,2]&Str1$[4,5]&Str2$[1,2]&Str2$[4,5]
473     PRINT "Default filename is ";F_name$
474     INPUT "Use this name (Y/N)?",Answ$
475     IF (Answ$="N" OR Answ$="n") THEN
476        INPUT "Enter filename of choice (max. 10):",F_name$
477     END IF
478     CREATE ASCII F_name$,100
479     ASSIGN @Path1 TO F_name$
480     PRINT "FILE ";F_name$;" CREATED."
481     INPUT "Add a comment to top of file (Y/N)?",Answ$
482     IF (Answ$="Y" OR Answ$="y") THEN
483        LINPUT "Type in message now:",String3$
484        OUTPUT @Path1;FNPr$(Dumm+1)&"Comment:  "&String3$
485        OUTPUT @Path1;FNPr$(Dumm+2)&Stars$
486        Dumm=Dumm+2
```

```
487    END IF
488    String3$=" "
489    F_flag=1
490 SUBEND
491  !
492  !
493 SUB Close_file
494    COM /File_info/ F_flag,Stars$,F_name$,@Path1,Dumm
495    ASSIGN @Path1 TO *
496    F_flag=0
497    GCLEAR
498    CLEAR SCREEN
499    PRINT "File ",F_name$," closed."
500 SUBEND
501  !
502  !
503 DEF FNPr$(Dumm)
504    String$=" "
505    String$=VAL$(Dumm)&"!   "
506    RETURN String$
507 FNEND
508  !
509 SUB Cal_line
510    COM /Line_loss/ Pstep,Pfrac,Pflag
511    COM /Values/ Fstart,Pwrl,Det_max
512    Pstep=0.
513    Pflag=1
514    PRINT "CONNECT TRANSMIT & RECEIVE CABLES TOGETHER W/O PROBE"
515  ! SET POWER LEVEL TO -5 DBM
516    Dum=Pwrl
517    Pwrl=-5
518    PRINT "THEN PRESS CONTINUE"
519    PAUSE
520    CALL Takedata
521    Dum2=1-Pfrac
522    Dbs=-10*LGT(Dum2)
523    Pstep=.01*Dbs
524      !Pstep=INT(Pstep/.006)*.006
525    PRINT "pstep",Pstep
526    Pflag=0
527    Pwrl=Dum
528    PRINT "SYSTEM IS NOW CALIBRATED FOR LINE ATTN."
529 SUBEND
530 !
531 !
532 SUB Rate
533    COM /Samp_rate/ Srate$[2]
534    INPUT "Select sampling mode (1=med, 2=fast):",Dum
535    SELECT Dum
536    CASE 1
537       Srate$="S1"
538    CASE 2
539       Srate$="S2"
540    CASE ELSE
541       BEEP
```

```
542       PRINT "Invalid Choice"
543       GOTO Choose2
544    END SELECT
545 SUBEND
```